第 48 卷 第 8 期/2021 年 4 月/中国激光 研究论文

中国激光

飞秒激光制备柔性纳米多孔 Ag 材料的研究

赵强[1]，万辉[1]，于圣韬[2]，栾世奕[2]，桂成群[1*]，周圣军[1,2**]

[1]武汉大学工业科学研究院，湖北 武汉 430072；

[2]武汉大学动力与机械学院，湖北 武汉 430072

摘要 柔性纳米多孔金属材料在柔性传感、柔性储能等领域具有巨大的应用前景。采用脱合金法、等离子体烧结法、热压法制备的纳米多孔金属材料具有较高的弹性模量和屈服强度，不能满足柔性器件的发展需求。为了解决该问题，通过采用高峰值功率的飞秒激光辐照具有良好柔韧性、导电性及抗氧化性银(Ag)纳米线的方法来制备柔性纳米多孔 Ag 材料。纳米压痕仪测试了柔性纳米多孔 Ag 材料的力学性能，实验结果表明，柔性纳米多孔 Ag 材料的力学性能随着飞秒激光辐照功率的增加而增强。此外，X 射线衍射仪测试了柔性纳米多孔 Ag 材料的晶粒尺寸，发现柔性纳米多孔 Ag 材料的晶粒尺寸随飞秒激光辐照功率的增大而减小。最后，对飞秒激光辐照法、脱合金法、等离子体烧结法、热压法制备的纳米多孔金属材料的屈服强度进行对比分析，当纳米多孔金属材料的晶粒尺寸为 50 nm 时，飞秒激光辐照制备的柔性纳米金属多孔材料屈服强度最小(0.8 Mpa)。

关键词 激光技术；柔性纳米多孔金属材料；飞秒激光；屈服强度；晶粒尺寸

中图分类号 TG456.7 **文献标志码** A **doi**：10.3788/CJL202148.0802009

1 引 言

纳米金属多孔材料具有大比表面积和高孔隙率的结构特点，在传感[1-4]和储能[5-8]等领域显示出了巨大的潜能。近年来，随着柔性电极、柔性传感器及柔性储能器件的快速发展[9-14]，需要制备出柔性纳米金属多孔材料。采用脱合金法、等离子体烧结法及热压法制备出的纳米多孔材料具有较高的弹性模量和屈服强度。例如，Wang 等[15]用脱合金法制备的纳米金属多孔材料的韧带尺寸为 100 nm 时，屈服强度大于 200 MPa。Fu 等[16]采用等离子体烧结银(Ag)纳米颗粒的方法，制备出了硬度大于 1.5 GPa 的纳米金属多孔材料。Peng 等[17]在 150 ℃高温环境、50 N 恒定压力条件下，采用热压方法有效合成了屈服强度趋近于理论数值(～2.6 GPa)的纳米多孔金属材料。为解决脱合金法、等离子体烧结法和热压法制备的纳米多孔金属材料的机械性能不能满足柔性器件应用需求的问题，本文介绍了飞秒激光辐照 Ag 纳米线制备柔性纳米金属多孔材料的方法。

Ag 纳米线具有良好的柔韧性、高的导电性、优异的抗氧化性等诸多优点，因此非常适合制作性能优异的柔性微纳器件[9-10, 18-24]。Cheong 等[9]采用烘箱加热的方法，将 Ag 纳米线制备成具有良好弯曲性能的混合透明导电电极。Chou 等[20]在 190 ℃的加热平台上制备了可用于高灵敏度传感器的柔性 Ag 纳米线图案。Park 等[10]采用闪光灯辐照 Ag 纳米线，合成了高输出电压和高输出电流密度的柔性透明能量器件。然而，无论是采用加热法还是采用闪光灯辐照法连接 Ag 纳米线时，都无法提供较强的局域能场，导致 Ag 纳米线交接处电阻过大。飞秒激光因为具有极短的脉冲宽度、超高的峰值功率等特点[25-30]，辐照金属纳米材料时，可形成超强的局域能场，使金属纳米材料在交接处充分熔融，从而解决了金属纳米材料在交接处电阻过大的问题。因此结合飞秒激光和 Ag 纳米线的优点，采用飞秒激光辐照 Ag 纳米线制备柔性纳米多孔 Ag 材料。

本文采用纳米压痕仪测量柔性纳米多孔 Ag 材

收稿日期：2020-12-01；**修回日期**：2021-01-02；**录用日期**：2021-02-23

基金项目：国家重点研发计划(2017YFB1104900)、国家自然科学基金(52075394，51675386，51775387)

* **E-mail**：cheng.gui.2000@gmail.com；** **E-mail**：zhousj@whu.edu.cn

料的弹性模量和屈服强度，采用 X 射线衍射仪(XRD)测试柔性纳米多孔 Ag 材料的晶粒尺寸。与脱合金法、等离子体烧结法及热压法制备纳米多孔金属材料的力学性能相比，飞秒激光辐照 Ag 纳米线制备的 Ag 纳米多孔材料的屈服强度最小。此外还分析了飞秒激光辐照功率对柔性纳米多孔 Ag 材料的晶粒尺寸和屈服强度的影响，实验结果表明，随着飞秒激光辐照功率的增大，柔性纳米多孔 Ag 材料的晶粒尺寸减小，屈服强度增大。

2　实　　验

柔性纳米多孔 Ag 材料的制备包括以下步骤：a)将 Ag 纳米线溶液和去离子水一并移入离心管；b)离心管置于超声波清洗仪中超声振荡，剥离覆盖在 Ag 纳米线表面的聚乙烯吡咯烷酮(PVP)；c)离心超声后的离心管，然后移除溶液表层的上清液，将高浓度的 Ag 纳米线浆料留在离心管底部，加入去离子水后，重复步骤 b)和步骤 c)数次，确保去除多余的 PVP；d)在室温下将高浓度的 Ag 纳米线浆料旋涂到硅衬底上；e)室温下把样品放在空气中静置，充分干燥硅基板上的 Ag 纳米线浆料；f)飞秒激光穿过透光片辐照干燥的 Ag 纳米线。在强烈的局部等离子体激元效应下 Ag 纳米线相互熔合，从而得到柔性纳米多孔 Ag 材料，如图 1 所示。分别设定激光辐照功率为 60，70，80，90，100 mW，可以获得 5 组纳米多孔 Ag 样品。

采用型号为 TCR-1030-10 的飞秒激光器制备柔性纳米多孔 Ag 材料，使用 TESCAN MIRA 3 LMH 场发射扫描电子显微镜(SEM)、FEI Titan G2 60-300 透射电子显微镜(TEM)及 KEYENCE VK-X100 三维共聚焦激光扫描显微镜(CLSM)进行表面形态表征，使用 Rigaku X 射线衍射仪来检测柔性纳米多孔 Ag 材料的晶粒尺寸。

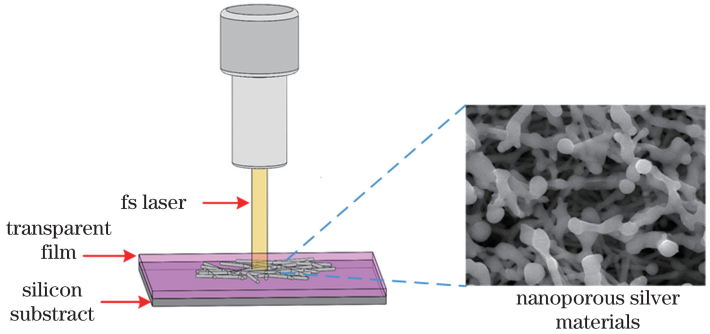

图 1　飞秒激光制备柔性纳米多孔材料示意图

Fig. 1　Schematic of flexible nanoporous materials fabricated by femtosecond laser

采用 Hysitron Ti -950 深度感应纳米压痕仪，配备 Berkovich 压头(泊松比为 0.07，弹性模量为 1141 GPa，半径约为 100 nm)来测量柔性金属纳米材料的屈服强度和弹性模量。实验中，选择加载速率为 30 μN/s 的恒定加载速率模式，再分别设定三个最大的峰值载荷 150，300，450 μN 来进行压痕实验。

3　分析与讨论

采用波长为 1030 nm，脉冲宽度为 800 fs 的飞秒激光，使用焦距为 70 mm 的场镜(飞秒激光设备由武汉虹拓新技术有限责任公司提供)。设定激光频率为 200 kHz，激光扫描速度为 1000 mm/s，扫描点中心间距为 10 μm，激光扫描路径间距为 10 μm。实验测量了 30 组 Ag 纳米线样品，得到了 Ag 纳米线的直径(300±30)nm 和长度(10±3)μm。飞秒激光制备的纳米多孔 Ag 材料样本标记为 FNAM-P，其中 FNAM 表示柔性纳米多孔 Ag 材料，P 表示制备柔性纳米多孔 Ag 材料的飞秒激光辐照功率。制备柔性纳米多孔 Ag 材料的飞秒激光辐照功率具体数值和对应参数如表 1 所示。

表 1　制备 FNAM 的飞秒激光辐照功率、激光辐照功率密度和相关标签

Table 1　Femtosecond laser irradiation power, irradiation power density, and related labels of prepared FNAM

Laser irradiation power /mW	0	60	70	80	90	100
Laser irradiation power density /(mW·cm^{-2})	0	0.76×10^{8}	0.89×10^{8}	1.02×10^{8}	1.15×10^{8}	1.27×10^{8}
FNAM-P	FNAM-0	FNAM-60	FNAM-70	FNAM-80	FNAM-90	FNAM-100

采用时域有限差分法(FDTD)模拟仿真 Ag 纳米线的电场分布，结合飞秒激光辐照 Ag 纳米线的

实验，分析 Ag 纳米线的熔化特性。选择高斯光源作为入射激光，设置入射激光的电矢量强度为 1 V/m，光源波长为 1030 nm。图 2(a)显示了电场在单根 Ag 纳米线和两根交叉 Ag 纳米线中的分布。可清晰得知：入射激光辐照单根 Ag 纳米线时，Ag 纳米线两端的电场强度最高；入射激光辐照两根交叉 Ag 纳米线时，Ag 纳米线交叉位置的电场强度最高。这种电场分布规律和局部表面等离子体激元共振规律一致。图 2(b)和(c)分别显示了不同飞秒激光强度下 Ag 纳米线的 SEM 图。飞秒激光辐照 Ag 纳米线时，Ag 纳米线局部表面等离子体激元共振最高处产生最强热量。当飞秒激光强度较小时，Ag 纳米线仅在搭接处熔化，形成纳米尺度互连，如图 2(b)所示。加大飞秒激光强度时，Ag 纳米线间隙部位熔融加剧，Ag 纳米线末端也开始熔化，并且 Ag 纳米线末端的线性结构逐渐向球状结构转变，如图 2(c)所示。从图 2 可知，实验结果和 FDTD 模拟仿真具有良好的一致性。

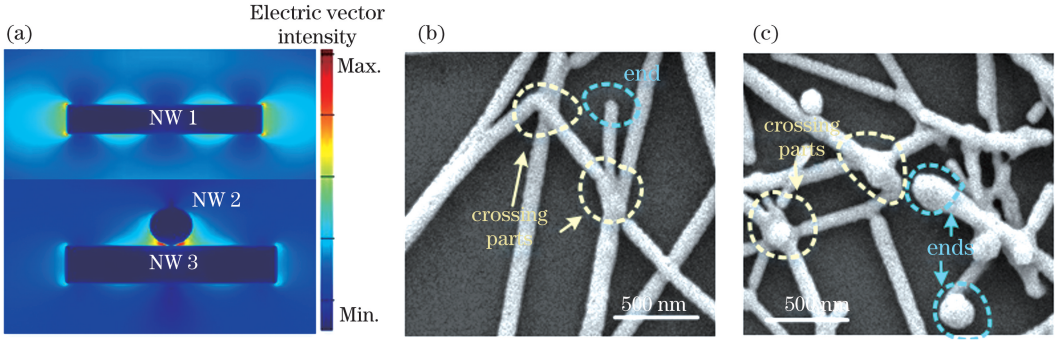

图 2　激光辐照下 Ag 纳米线(NW)的能场分布及形貌变化。(a)电场在单根 Ag 纳米线和两根交叉 Ag 纳米线上的分布；(b)适量飞秒激光功率辐照时，Ag 纳米线相互连接的 SEM 图；(c)过量飞秒激光辐照时，Ag 纳米线相互连接的 SEM 图

Fig. 2　Electric field distribution and morphological changes of Ag nanowires irradiated by fs laser. (a) Electric field distribution at a single Ag nanowire (AgNW) and two crossing AgNWs; (b) SEM image of AgNWs connected to each other irradiated by moderate fs laser power; (c) SEM image of AgNWs connected to each other irradiated by excessive fs laser power

图 3(a)显示了飞秒激光辐照前 Ag 纳米线的 SEM 图，图 3(b)～(f)分别显示了 60，70，80，90，100 mW 激光功率辐照下 Ag 纳米线的 SEM 图。当飞秒激光为 60 mW 时，Ag 纳米线局部熔化，与相邻纳米线产生互连，如图 3(b)所示。随着飞秒激光辐照功率的增大，Ag 纳米线熔化程度加剧，纳米互连结构的体积和数量增加，并且在纳米线末端有明显的球状结构产生，如图 3(c)～(f)所示。

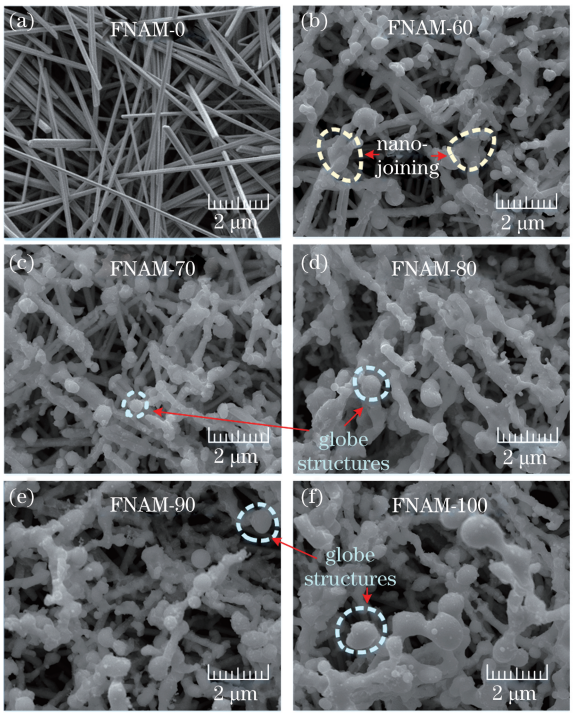

图 3　Ag 纳米材料的 SEM 图像。(a)未被飞秒激光辐照 Ag 纳米线的 SEM 图像；(b)～(f)飞秒激光功率为 60，70，80，90，100 mW 时，柔性纳米多孔 Ag 材料的 SEM 图像

Fig. 3　SEM images of silver nanomaterials. (a) SEM image of unirradiated silver nanowires; (b)-(f) SEM images of flexible nanoporous silver materials irradiated by different laser irradiation powers of 60, 70, 80, 90, 100 mW

图 4 描述了纳米压痕实验中载荷与压痕深度的对应曲线。采用带有 Berkovich 压头的纳米压痕仪测试了飞秒激光制备柔性纳米多孔 Ag 材料的力学性能，分别设定了三个峰值压力 150，300，450 μN，如图 4(a)所示。图 4(b)和(c)是柔性纳米多孔 Ag 材料上残留纳米压痕对应的 CLSM 图，可以观察到，塑性变形仅发生在残余压痕区域，残余压痕的相邻区域未出现材料堆积或材料变形情况，这表明 Berkovich 压头下的纳米多孔 Ag 材料发生了局部致密化。

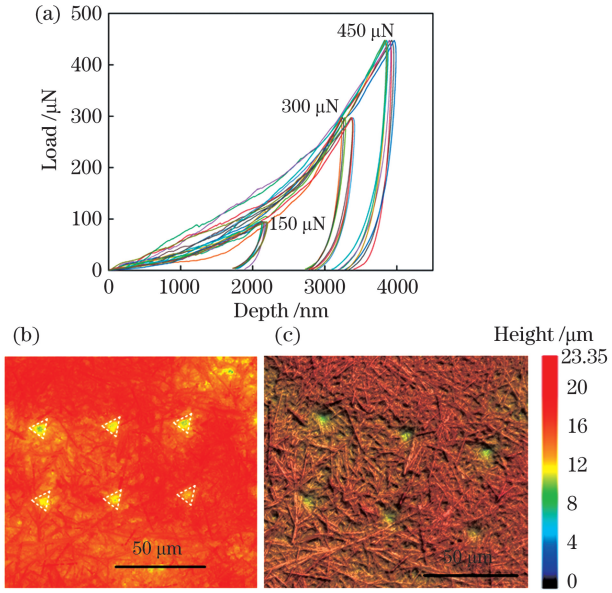

图 4　柔性纳米多孔 Ag 材料的纳米压痕实验。(a)使用 Berkovich 压头的系列载荷与压痕深度的曲线；(b)残留压痕高度信息的 CLSM 图；(c)包含残留压痕颜色和激光光量信息的 CLSM 图

Fig. 4　Nanoindentation experiments of flexible nanoporous silver materials. (a) Serious of load versus depth using a Berkovich tip; (b) CLSM image of residual indentation containing the information of height; (c) CLSM image of residual indentation containing the information of color and laser light quantity information

图 5(a)显示了聚焦离子束(FIB)刻蚀柔性纳米多孔 Ag 材料的原位 SEM 图。FIB 刻蚀后，柔性纳米多孔 Ag 材料被减薄至 54 nm。图 5(b)和(c)分别显示了柔性纳米多孔 Ag 材料薄膜的俯视图和主视图，可以明确得知柔性纳米多孔 Ag 材料的取样位置。图 5(d)显示了图 5(c)中标记区域放大的 TEM 图，右上角对应的是快速傅里叶变换(FFT)图。从放大的 TEM 图和 FFT 图中可以清晰地观察到柔性纳米多孔 Ag 材料的晶格。因此可以得出结论：激光辐照后，纳米 Ag 单晶材料转变为纳米 Ag 多晶材料，柔性纳米多孔 Ag 材料的晶格呈现多晶特性。采用 Rigaku X 射线衍射仪，分别测试了实验制备的 5 组柔性纳米多孔 Ag 材料，图 5(e)显示了 5 组柔性纳米多孔 Ag 材料的 XRD 图。还采用 XRD 衍射仪测试了这 5 组柔性纳米多孔 Ag 材料的晶粒尺寸数据。图 5(f)显示了这 5 组柔性纳米多孔 Ag 材料的晶粒尺寸和激光辐照功率的关系，即柔性纳米多孔 Ag 材料的晶粒尺寸随着飞秒激光辐照功率的增大而减小。当飞秒激光辐照功率为 60 mW 时，柔性纳米多孔 Ag 材料的晶粒尺寸为 44.6 nm；当飞秒激光辐照功率为 100 mW 时，柔性纳米多孔 Ag 材料的晶粒尺寸为 41.5 nm。

由于纳米多孔 Ag 材料发生了局部致密化，所以此时纳米压痕实验如同单轴压缩实验，屈服强度

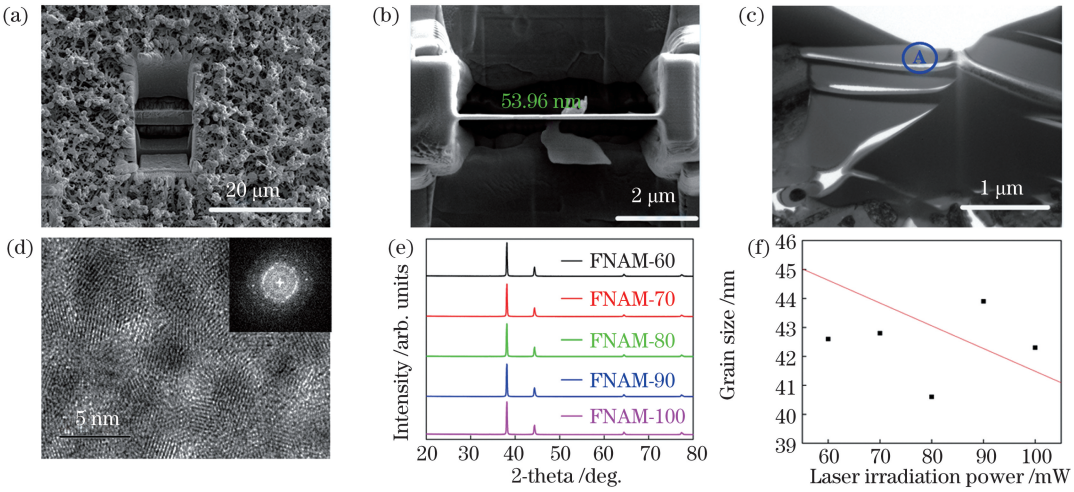

图 5　激光辐照对柔性纳米多孔 Ag 材料晶体变化的影响。(a)FIB 刻蚀柔性纳米多孔 Ag 材料的 SEM 图；(b) FIB 刻蚀后，柔性纳米多孔 Ag 材料薄膜的俯视图；(c)柔性纳米多孔 Ag 材料的截面图；(d)图 5(c)标记部分的 TEM 图，插图是 FFT 图；(e)不同飞秒激光辐照功率下柔性纳米多孔 Ag 材料的 XRD 图谱；(f)柔性纳米多孔 Ag 材料的晶粒尺寸和激光辐照功率的关系

Fig. 5　Effect of laser irradiation on crystal changes of flexible nanoporous silver materials. (a) SEM image of flexible nanoporous silver materials lifted off by FIB; (b) top view of flexible nanoporous silver materials film thinned after FIB milling; (c) cross-sectional view of flexible nanoporous silver materials; (d) TEM image corresponding to the area marked in Fig. 5(c), inset shows the corresponding FFT pattern; (e) XRD patterns of flexible nanoporous silver materials irradiated by different fs laser irradiation power; (f) grain size versus laser irradiation power of flexible nanoporous silver materials

σ 和硬度数值 H 近似相等[31]，即 $\sigma \approx H$，该公式可用来描述可压缩纳米多孔 Ag 材料的力学特性。

图 6(a)描述了柔性纳米多孔 Ag 材料的弹性模量和飞秒激光辐照功率的关系，图 6(b)描述了柔性纳米多孔 Ag 材料的屈服强度和飞秒激光辐照功率的关系。可以看出：随着激光辐照功率的增大，柔性纳米多孔材料的弹性模量和屈服强度都呈现上升趋势；在 450 μN 的峰值负载下，FNAM-100 的弹性模量(235.2 MPa)是 FNAM-60 弹性模量(88.4 MPa)的 2.66 倍，FNAM-100 的屈服强度(2551.6 kPa)是 FNAM-60 屈服强度(1102.0 kPa)的 2.32 倍。飞秒激光辐照功率越强，Ag 纳米单晶转变为 Ag 纳米多晶的粒径就越小，相同面积下晶界的数目就越多。晶界可以有效地阻碍晶体因受力而出现的位错滑移，晶界数目越多，阻碍位错滑移的能力就越强，因而柔性纳米多孔 Ag 材料的弹性模量和屈服强度就越大。

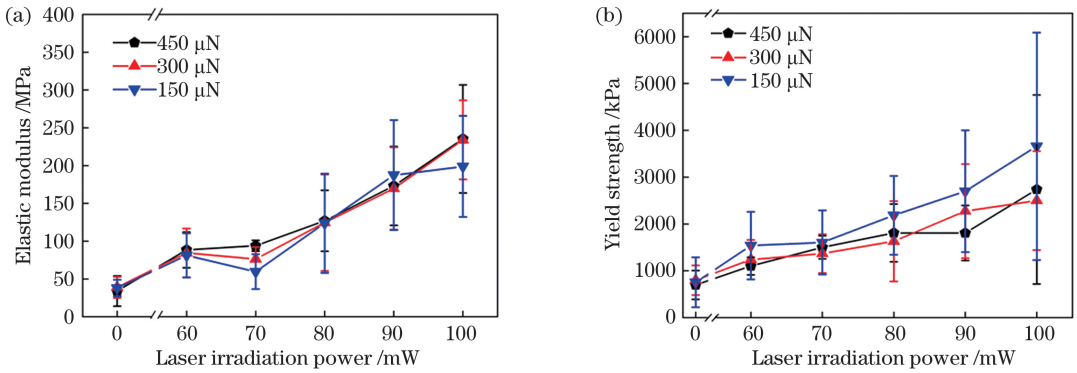

图 6　柔性纳米多孔 Ag 材料的力学性能。(a)弹性模量与激光辐照功率的关系；(b)屈服强度与激光辐照功率的关系

Fig. 6　Mechanical properties of flexible nanoporous silver materials. (a) Elastic modulus versus laser irradiation power; (b) yield strength versus laser irradiation power

图 7 描述了本研究制备的柔性纳米多孔 Ag 材料屈服强度和他人制备的纳米多孔金属材料屈服强度的对比关系。横轴代表纳米多孔金属材料的晶粒尺寸，纵轴代表纳米多孔金属材料的屈服强度。当晶粒尺寸为 50 nm 时，本研究制备的柔性纳米多孔 Ag 材料的屈服强度为 0.8 MPa，与 Peng 等使用高温热压 Ag 纳米线的方法[17]制备的纳米多孔 Ag 材料的屈服强度 1237.3 MPa 相比，仅为其 0.065%；与 Caro 等使用脱合金法[32]制备的纳米多孔金材料的屈服强度 719.6 MPa 相比，为其 0.11%；与 Fu 等使用等离子体烧结 Ag 纳米颗粒的方法[16]制备的纳米多孔 Ag 材料的屈服强度 492.9 MPa 相比，为其 0.16%；与 Wang 等使用脱合金法[15]制备的纳米多孔金材料的屈服强度 142.3 MPa 相比，为其 0.56%。以上结果表明，飞秒激光辐照 Ag 纳米线制备的柔性纳米多孔 Ag 材料的屈服强度(硬度)最小。

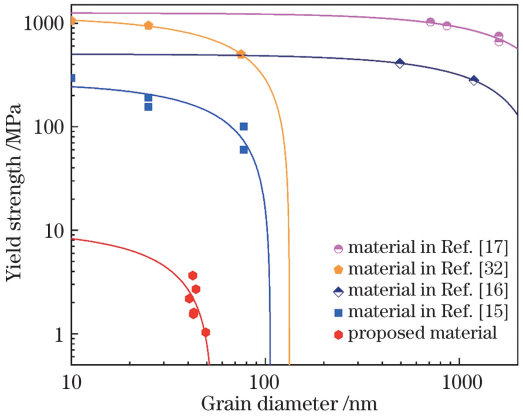

图 7　纳米多孔 Ag 材料的屈服强度与晶粒尺寸的关系

Fig. 7　Yield strength of nanoporous Ag materials versus grain size

4　结　　论

采用飞秒激光辐照 Ag 纳米线的方法制备了柔性纳米多孔 Ag 材料。通过纳米压痕仪分析了飞秒激光对柔性纳米多孔 Ag 材料力学性能的影响，X 射线衍射仪测试了柔性纳米多孔材料的晶粒尺寸变化。纳米多孔 Ag 材料的弹性模量和屈服强度随激光辐照功率的增大而增加。在 450 μN 峰值负载下，飞秒激光辐照功率从 60 mW 增大至 100 mW 时，纳米多孔 Ag 材料的弹性模量从 88.4 MPa 增大至 235.2 MPa，屈服强度从 1102.0 MPa 增大至 2737.0 MPa。纳米多孔 Ag 材料的晶粒尺寸随激光功率的增加而减小。飞秒激光辐照功率从 60 mW 增大至 100 mW 时，纳米多孔 Ag 材料的晶粒尺寸从 44.6 nm 减小至 41.5 nm。相同晶粒尺寸条件下，与热压法、等离子体烧结法、脱合金法相比，飞秒

激光辐照 Ag 纳米线制备的柔性纳米多孔 Ag 材料的屈服强度最低。

参 考 文 献

[1] Zhang L, Chang H X, Hirata A, et al. Nanoporous gold based optical sensor for sub-ppt detection of mercury ions[J]. ACS Nano, 2013, 7(5): 4595-4600.

[2] Zhang J, Li C M. Nanoporous metals: fabrication strategies and advanced electrochemical applications in catalysis, sensing and energy systems [J]. Chemical Society Reviews, 2012, 41(21): 7016-7031.

[3] Mathesan S, Mordehai D. Size-dependent elastic modulus ofnanoporous Au nanopillars [J]. Acta Materialia, 2020, 185: 441-452.

[4] Gwak E J, Jeon H, Song E, et al. Twinned nanoporous gold with enhanced tensile strength[J]. Acta Materialia, 2018, 155: 253-261.

[5] Lang X Y, Hirata A, Fujita T, et al. Nanoporous metal/oxide hybrid electrodes for electrochemical supercapacitors[J]. Nature Nanotechnology, 2011, 6(4): 232-236.

[6] Liu Z, Chuah C S L, Scanlon M G. Compressive elastic modulus and its relationship to the structure of a hydrated starch foam[J]. Acta Materialia, 2003, 51(2): 365-371.

[7] Gibson L J. Mechanical behavior of metallic foams [J]. Annual Review of Materials Science, 2000, 30(1): 191-227.

[8] Fujita T, Kanoko Y, Ito Y, et al. Nanoporous metal papers for scalable hierarchical electrode [J]. Advanced Science, 2015, 2(8): 1500086.

[9] Cheong H G, Triambulo R E, Lee G H, et al. Silver nanowire network transparent electrodes with highly enhanced flexibility by welding for application in flexible organic light-emitting diodes [J]. ACS Applied Materials & Interfaces, 2014, 6(10): 7846-7855.

[10] Park J H, Hwang G T, Kim S, et al. Flash-induced self-limited plasmonic welding of silver nanowire network for transparent flexible energy harvester[J]. Advanced Materials, 2017, 29(5): 1603473.

[11] Fu X M, Xu L M, Li J X, et al. Flexible solar cells based on carbon nanomaterials[J]. Carbon, 2018, 139: 1063-1073.

[12] Park J, Hwang J C, Kim G G, et al. Flexible electronics based on one-dimensional and two-dimensional hybrid nanomaterials [J]. InfoMat, 2020, 2(1): 33-56.

[13] Kamyshny A, Magdassi S. Conductive nanomaterials for 2D and 3D printed flexible electronics [J]. Chemical Society Reviews, 2019, 48(6): 1712-1740.

[14] Yao S S, Ren P, Song R Q, et al. Nanomaterial-enabled flexible and stretchable sensing systems: processing, integration, and applications [J]. Advanced Materials, 2020, 32(15): 1902343.

[15] Wang K, Kobler A, Kübel C, et al. Nanoporous-gold-based composites: toward tensile ductility [J]. NPG Asia Materials, 2015, 7(6): e187.

[16] Fu Y Q, Shearwood C, Xu B, et al. Characterization of spark plasma sintered Ag nanopowders [J]. Nanotechnology, 2010, 21(11): 115707.

[17] Peng P, Sun H, Gerlich A P, et al. Near-ideal compressive strength ofnanoporous silver composed of nanowires[J]. Acta Materialia, 2019, 173: 163-173.

[18] Chen Y T, Carmichael R S, Carmichael T B. Patterned, flexible, and stretchable silver nanowire/polymer composite films as transparent conductive electrodes[J]. ACS Applied Materials & Interfaces, 2019, 11(34): 31210-31219.

[19] Mao Y Y, Ji B, Chen G, et al. Robust and wearable pressure sensor assembled from AgNW-coated PDMS micropillar sheets with high sensitivity and wide detection range[J]. ACS Applied Nano Materials, 2019, 2(5): 3196-3205.

[20] Chou N, Kim Y, Kim S. A method to pattern silvernanowires directly on wafer-scale PDMS substrate and its applications [J]. ACS Applied Materials & Interfaces, 2016, 8(9): 6269-6276.

[21] Wang S, Gong L P, Shang Z J, et al. Novel safeguarding tactile e-skins for monitoring human motion based on SST/PDMS-AgNW-PET hybrid structures[J]. Advanced Functional Materials, 2018, 28(18): 1707538.

[22] Chen W H, Li F W, Liou G S. Novel stretchable ambipolar electrochromic devices based on highly transparent AgNW/PDMS hybrid electrodes [J]. Advanced Optical Materials, 2019, 7(19): 1900632.

[23] Fan H W, Li K R, Li Q, et al. Prepolymerization-assisted fabrication of an ultrathin immobilized layer to realize a semi-embedded wrinkled AgNW network for a smart electrothermal chromatic display and actuator [J]. Journal of Materials Chemistry C, 2017, 5(37): 9778-9785.

[24] Madeira A, Plissonneau M, Servant L, et al. Increasing silver nanowire network stability through small molecule passivation[J]. Nanomaterials, 2019, 9(6): 899.

[25] Keller U. Recent developments in compact ultrafast lasers[J]. Nature, 2003, 424(6950): 831-838.

[26] Liao J N, Wang X D, Zhou X W, et al. Femtosecond laser direct writing of copper microelectrodes[J]. Chinese Journal of Lasers, 2019, 46(10): 1002013.
廖嘉宁, 王欣达, 周兴汶, 等. 飞秒激光直写铜微电极研究[J]. 中国激光, 2019, 46(10): 1002013.

[27] Long J, Jiao B Z, Fan X H, et al. Femtosecond laser assembly of one-dimensional nanomaterials and their application[J]. Chinese Journal of Lasers, 2021, 48(2): 0202017.
龙婧, 焦玢璋, 范旭浩, 等. 飞秒激光组装一维纳米材料及其应用[J]. 中国激光, 2021, 48(2): 0202017.

[28] Shi Y, Xu B, Wu D, et al. Research progress on fabrication of functional microfluidic chips using femtosecond laser direct writing technology[J]. Chinese Journal of Lasers, 2019, 46(10): 1000001.
史杨, 许兵, 吴东, 等. 飞秒激光直写技术制备功能化微流控芯片研究进展[J]. 中国激光, 2019, 46(10): 1000001.

[29] Lu M J, Wu T, Li Y, et al. Dual-comb nonlinear spectroscopy[J]. Laser & Optoelectronics Progress, 2021, 58(1): 0100001.
卢敏健, 武韬, 李岩, 等. 双光梳非线性光谱[J]. 激光与光电子学进展, 2021, 58(1): 0100001.

[30] Yu D, Sun Y, Feng Z S, et al. Improving emission intensity of femtosecond laser-induced breakdown spectroscopy by using circular polarization[J]. Chinese Journal of Lasers, 2021, 48(1): 0111001.
于丹, 孙艳, 冯志书, 等. 通过圆偏振光提高飞秒激光诱导击穿光谱的发射强度[J]. 中国激光, 2021, 48(1): 0111001.

[31] Biener J, Hodge A M, Hamza A V, et al. Nanoporous Au: a high yield strength material[J]. Journal of Applied Physics, 2005, 97(2): 024301.

[32] Caro M, Mook W M, Fu E G, et al. Radiation induced effects on mechanical properties ofnanoporous gold foams[J]. Applied Physics Letters, 2014, 104(23): 233109.

Investigation of Flexible Nanoporous Silver Materials Fabricated by Femtosecond Laser

Zhao Qiang[1], Wan Hui[1], Yu Shengtao[2], Luan Shiyi[2], Gui Chengqun[1*], Zhou Shengjun[1,2**]

[1] *The Institute of Technological Sciences, Wuhan University, Wuhan, Hubei* 430072, *China*;

[2] *School of Power and Machinery, Wuhan University, Wuhan, Hubei* 430072, *China*

Abstract

Objective Owing to high porosity and large specific surface areas, nanoporous metal materials have attracted considerable attention for applications in sensors, energy storage, etc. With the rapid development of flexible sensors and energy storage devices, the fabrication of flexible nanoporous metal materials is becoming more and more important in recent years. However, nanoporous metal materials prepared by dealloying, spark plasma sintering, and heat pressing exhibit an extremely high elastic modulus and yield strength that do not meet the requirements of flexible devices. To overcome these problems, herein, flexible nanoporous metal materials were prepared by irradiating Ag nanowires (NWs) using a femtosecond (fs) laser.

Ag NWs are ideal nanomaterials for fabricating flexible nanoporous metal materials because of their good flexibility, conductivity, and oxidation resistance. The fs laser offers several advantages such as ultrashort pulse width and ultrahigh peak power. Flexible nanoporous metal materials prepared by irradiating Ag NWs using the fs laser show ultralow yield strength, which can meet the requirements of flexible devices. In this study, a novel method for preparing flexible nanoporous silver materials is reported and the influence of fs laser power on the yield strength of the resulting flexible nanoporous Ag materials is revealed.

Methods The following steps are involved in the fabrication process of flexible nanoporous Ag materials. The as-synthesized Ag NW solution and deionized (DI) water were pipetted into a centrifuge tube using a pipettor. Then, the centrifuge tube containing the Ag NWs solution and DI water was placed in an ultrasonic cleaner to strip the polyvinylpyrrolidone (PVP) coating the surface of Ag NWs. Subsequently, the centrifuge tube was centrifuged to obtain highly concentrated Ag NW pastes. After adding DI water, ultrasound and centrifugation were performed several times to remove excess PVP. The Ag NW paste was dropped onto a silicon substrate and completely dried at room temperature. Then, the dried Ag NWs were irradiated using the fs laser to fabricate the flexible nanoporous Ag materials. Nanoindentation experiments were performed to analyze the mechanical properties of the as-prepared

flexible nanoporous Ag material. X-ray diffractometer (XRD) and high-resolution transmission electron microscopy were used to analyze the crystalline structure of the flexible nanoporous Ag materials. Additionally, the yield strength of nanoporous metal materials fabricated using different methods was compared.

Results and Discussions The fs laser irradiation of nanowires can induce localized surface plasmon resonance on the Ag NW surface. When the intensity of the fs laser is low, nanojoining occurs owing to the melting of the Ag NWs at the contact region. By increasing the intensity of the fs laser, the ends of the Ag NWs begin to melt and the linear ends of Ag NWs gradually transform into a spherical structure (Fig. 2). When the fs laser power is 60 mW, nanojoining occurs at the gaps between the Ag NWs because of local fusion. The volume and number of nanojoining increase with an increase in the fs laser power, and spherical structures are observed at the end of Ag NWs (Fig. 3). The yield strength of flexible nanoporous Ag materials is determined using depth-sensing nanoindentation equipped with a Berkovich indenter. Different peak loads (150, 300, and 450 μN) are investigated. Plastic deformation is found to only occur at the residual indentation impression, and no nanoporous material deformation adjacent to the contact impression is observed. This result indicates the occurrence of significant densification of the flexible nanoporous Ag materials under the Berkovich indenter (Fig. 4). With increasing fs laser power, the elastic modulus and yield strength of flexible nanoporous Ag materials increase, while their grain size decreases (Fig. 6). The yield strength of flexible nanoporous metal materials prepared using different methods is compared in this study. The experimental data clearly show that nanoporous Ag materials prepared using the fs laser exhibit the smallest yield strength at the same grain size (Fig. 7).

Conclusions The flexible nanoporous Ag materials are prepared by irradiating Ag NWs using the fs laser. The mechanical properties and grain size of the synthesized flexible nanoporous Ag materials are evaluated using a nanoindenter and XRD, respectively. Based on the experimental results, several important conclusions can be drawn.

1) The elastic modulus and yield strength of nanoporous Ag materials increase with an increase in the fs laser power. At a peak load of 450 μN and when the fs laser power is increased from 60 to 100 mW, the elastic modulus and yield strength of the flexible nanoporous Ag materials increase from 88.4 to 235.2 MPa and from 1102.0 to 2737.0 MPa, respectively.

2) The grain size of the flexible nanoporous Ag materials decreases with an increase in the fs laser power. When the fs laser power is increased from 60 to 100 mW, the grain size decreases from 44.6 to 41.5 nm.

3) Compared with Ag materials prepared by hot pressing, plasma sintering, and dealloying, flexible nanoporous Ag materials prepared by irradiating Ag NWs using the fs laser exhibit the lowest yield strength at the same grain size.

Key words laser technique; flexible nanoporous metal material; femtosecond laser; yield strength; grain size

OCIS codes 140.3390; 160.4236; 230.4000